In-beam spectroscopic study of ^{63}Zn

U. S. Ghosh,[1] S. Rai,[1,2] B. Mukherjee,[1,*] A. Biswas,[1] A. K. Mondal,[1] K. Mandal,[1] A. Chakraborty,[1] S. Chakraborty,[3] G. Mukherjee,[4] A. Sharma,[5] I. Bala,[6] S. Muralithar,[6] and R. P. Singh[6]

[1]*Department of Physics, Siksha-Bhavana, Visva-Bharati, Santiniketan, Bolpur - 731235, India*
[2]*Department of Physics, Salesian College, Siliguri Campus, Siliguri - 734001, India*
[3]*Department of Physics, Institute of Science, Banaras Hindu University, Varanasi - 221005, India*
[4]*Variable Energy Cyclotron Centre, 1/AF Bidhannagar, Kolkata - 700064, India*
[5]*Department of Physics, Himachal Pradesh University, Shimla-171005, India*
[6]*Inter University Accelerator Centre, Aruna Asaf Ali Marg, New Delhi - 110067, India*

(Received 15 March 2019; revised manuscript received 21 July 2019; published 16 September 2019)

Investigation on the excited states of ^{63}Zn was done through in-beam γ-ray spectroscopic techniques using the ^{52}Cr(^{18}O, $\alpha 3n$) fusion-evaporation reaction at a beam energy of 72.5 MeV. Detection of the emitted γ rays from the excited nuclei was performed in the coincidence mode using 14 Compton suppressed Ge clover detectors of the Indian National Gamma Array. Based on the γ-γ coincidence data, 13 new transitions have been placed in the level scheme following their coincidence relationship and intensity balance. Spin and parity assignments of the excited levels have been carried out by extracting the directional correlation from oriented states ratio and polarization asymmetry values of the emitted γ rays. Shell model calculations have been performed in the $f_{5/2}pg_{9/2}$ model space with a ^{56}Ni core using the jj44bpn interaction, to interpret the observed excited states of the nucleus. A reasonable agreement is found between the experimental findings and the shell-model calculations. In order to understand the evolution of a collective shape built on the $9/2^+$ (1704 keV) state, we have performed total Routhian surface calculations with a $1g_{9/2}$ quasineutron and found reasonable agreement.

DOI: 10.1103/PhysRevC.100.034314

I. INTRODUCTION

Nuclear structure in $A \approx 60$ reveals both single particle and collective excitations with various competing shapes, namely, prolate, oblate, and triaxial. A striking interplay of single particles and collective degrees of freedom have been observed in many Ge [1–5] and Cu [6–10] isotopes in this region. Here, the active orbitals are $2p_{3/2}$, $1f_{5/2}$, $2p_{1/2}$ in the upper fp shell and the intruder $1g_{9/2}$ orbital. The lower excitations are due to the negative parity $2p_{3/2}$, $1f_{5/2}$, and $2p_{1/2}$ orbitals but most of the high spin states are mainly due to the presence of the high-j $1f_{7/2}$ and $1g_{9/2}$ orbitals. The coupling of the $1g_{9/2}$ orbital with $2p_{3/2}$ orbital gives rise to the onset of octupole correlation. Strutinsky-type potential energy calculations by Nazarewicz *et al.* predicted softness toward octupole correlations for nuclei with $N, Z \approx 34$ [11,12]. Presence of holes in $1f_{7/2}$ orbital and particles in $1g_{9/2}$ orbital leads to a transition from spherical toward deformed shapes and enhances the possibility of collective rotational excitations. A magic superdeformed band in $N = Z$ ^{60}Zn was first observed by Svensson *et al.* [13] and spin-parity, excitation energy of the superdeformed states in this band were measured first by identifying linking transitions connecting this band to the yrast line. Among ^{61,63,65}Zn isotopes, the structure of ^{61}Zn is very interesting as several normal and superdeformed bands have been observed in this nucleus at high spins [14–16]. Strongly coupled rotational band was first observed in ^{64}Zn [17,18] in this mass region and this band shows similar characteristics of those smoothly terminating rotational bands in the Sn-Sb nuclei of the $A \approx 110$ region [19]. The lowest collective band in ^{64}Zn was interpreted as based on the $\pi(f_{7/2})^{-1}(p_{3/2}f_{5/2})^2(g_{9/2})^1\nu(p_{3/2}f_{5/2})^4(g_{9/2})^2$ configuration. The structure of ^{62}Zn also draws attention as it was the first candidate in this mass region in which the superdeformed band was observed with a large deformation ($\beta_2 \approx 0.45$) [20]. Later, extended study on this isotope revealed two sets of strongly coupled rotational bands observed up to the terminating states of their respective configurations [21]. A milestone in more extensive study of the structure of ^{62}Zn was achieved by Gellanki *et al.* [22], which established ten new rotational bands along with two new superdeformed bands and extended the level scheme above 40 MeV in excitation energy. Similarly two highly deformed and one superdeformed bands in ^{65}Zn were established by Yu *et al.* [23]. A rotational band was also observed in ^{65}Zn, built on $1g_{9/2}$ neutron orbital which exhibits a band crossing at high rotational frequency [24]. In ^{60,61,62,64,65}Zn, phenomena, like collective excitations including superdeformations, are reported to be due to a limited number of holes in the $1f_{7/2}$ subshell and excitation of one or more nucleons into $1g_{9/2}$ intruder orbitals above the ^{56}Ni core.

Previous investigations on medium and high spin states in ^{63}Zn were performed using proton, α, ^{12}C, ^{16}O, and deuteron beams [25–29]. The latest study with ^{16}O beam was done using 12 Compton suppressed HPGe detectors along with 14

*buddhadev.mukherjee@visva-bharati.ac.in

BGO detectors [28]. Singh *et al.* established a positive parity unfavored and a negative parity favored band in ^{63}Zn. The band head of the positive parity band is $9/2^+$ which couples with the excited vibrational core of ^{62}Zn producing higher excited positive parity states. The higher excited $13/2^+_1$, $17/2^+$, and $21/2^+$ states decay to the band head via the cascade of strong stretched electric quadrupole ($E2$) transitions. Here, we report on an experiment that was carried out with a comparatively efficient array to bring out more comprehensive knowledge on the high spin nuclear structure in ^{63}Zn.

II. EXPERIMENTAL DETAILS AND DATA ANALYSIS

In the fusion-evaporation reaction a beam of ^{18}O at 72.5 MeV was obtained from the 15-UD pelletron accelerator [30] at Inter University Accelerator Centre (IUAC), New Delhi. The beam was bombarded onto a ^{52}Cr (isotopic abundance ≈99%) target of thickness 1.0 mg/cm^2 backed by 8.0 mg/cm^2 ^{197}Au. The emitted γ rays were detected in coincidence mode with 14 Compton suppressed HPGe clover detectors of the Indian National Gamma Array (INGA) [31]. Out of the 14 clovers, four were kept at an angle of 123° and another four at 148°, while the remaining six were placed at an angle of 90° with respect to the beam direction. The detectors were kept at a distance of ≈25 cm from the target. Further details of the experiment can be found in Ref. [32,33]. Analysis of the data is performed with the help of the standard analysis packages viz. CANDLE [34], RADWARE [35], and INGASORT [36]. Angular correlation analysis is carried out using the method of directional correlation from oriented states (DCO) [37]. In the present INGA geometry, the DCO ratios ($R_{\rm DCO}$) are obtained from the intensity ratios of the coincident events detected at the angles of 148° and 90° with respect to the beam direction. The DCO ratio is obtained from the formula

$$R_{\rm DCO} = \frac{I_{\gamma_1} \text{ at } 148^\circ \text{ gated by } \gamma_2 \text{ at } 90^\circ}{I_{\gamma_1} \text{ at } 90^\circ \text{ gated by } \gamma_2 \text{ at } 148^\circ}, \quad (1)$$

where I_{γ_1} is the measured intensity of γ_1 when the gating transition is γ_2. The expected $R_{\rm DCO}$ values for the stretched quadrupole and the dipole transitions are ≈1.0(2.0) and ≈0.5(1.0), for a pure quadrupole (dipole) gate. Here, in this work we measured DCO ratios from gates on 882 keV ($\frac{13}{2}^+ \rightarrow \frac{9}{2}^+$) and 1063 keV ($\frac{7}{2}^- \rightarrow \frac{3}{2}^-$) $E2$ and 640 keV ($\frac{9}{2}^+ \rightarrow \frac{7}{2}^-$) $E1$ transitions of ^{63}Zn. Measured DCO values of different transitions as obtained in this work are plotted in Fig. 1. The clover detector can be used as a Compton polarimeter [38–41] as it has closed geometry and using this facility the asymmetry in polarization of the Compton scattered photons was extracted to define electric or the magnetic nature of the γ-ray transitions from the coincidence data. Two asymmetric matrices were constructed from the coincidence data, with events corresponding to the single hits in any detector along one axis and the double-hit scattered events of the 90° detector on the other axis. The scattered events are either parallel or perpendicular, the asymmetry parameter is evaluated as

$$\Delta_{\rm asym} = \frac{a(E_\gamma)N_\perp - N_\parallel}{a(E_\gamma)N_\perp + N_\parallel}, \quad (2)$$

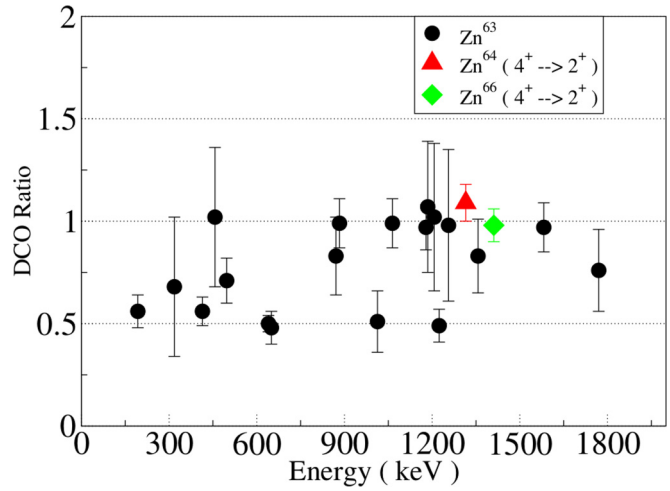

FIG. 1. DCO ratios of different transitions belonging to ^{63}Zn (gated by the $E2$ and $E1$ transitions, as mentioned in Table I). DCO ratios of the $4^+ \rightarrow 2^+$ transitions in ^{64,66}Zn gated by their respective $2^+ \rightarrow 0^+$ transitions, populated in the same reaction, are also presented for comparison. Please see Table I for details.

where $a(E_\gamma)$ is the asymmetry correction factor, representing the geometrical asymmetry of the present INGA setup and was determined from the ratio of the parallel ($N_\parallel$) and the perpendicular ($N_\perp$) scattered events obtained from an unpolarized source. It is defined as

$$a(E_\gamma) = \frac{N_\parallel(\text{unpolarized})}{N_\perp(\text{unpolarized})}. \quad (3)$$

The value of the asymmetry correction factor for the present detector setup is found to be ≈1.03(2) in the energy range ≈0.1–1.5 MeV using the standard ^{152}Eu radioactive source. Figure 2 shows the variation of the asymmetry correction factor within the γ-ray energy range ≈200–1500 keV for one

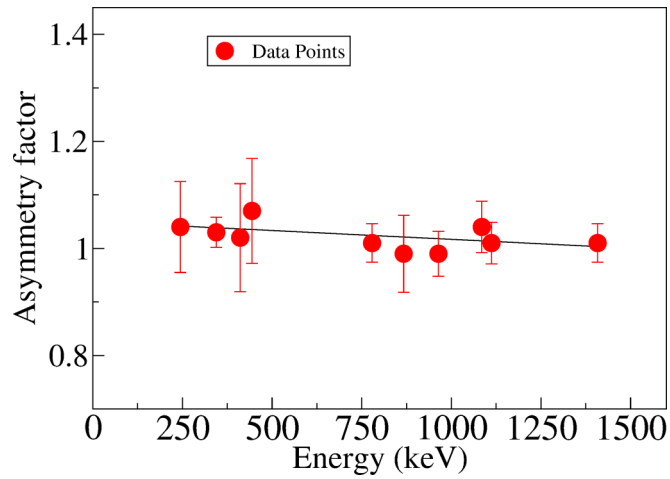

FIG. 2. Plot of asymmetry correction factor in the γ-ray energy range ≈200–1500 keV. Data points are fitted using the equation $a_0E_\gamma + a_1$, where $a_1 = 1.044(17)$, $a_0 = -3.311 \times 10^{-5}$, and E_γ is the energy of the γ ray. This is measured using the radioactive ^{152}Eu source for one of the 90° clover detectors used in the present setup.

TABLE I. Values of the level energies (E_i) in keV, γ-ray energies (E_γ) in keV, initial (I_i^π) $\rightarrow$ final (I_f^π) spin (in $\hbar$) parity, relative intensities (I_γ), branching ratio (B.R.), DCO ratio ($R_{\rm DCO}$), and polarization asymmetry ($\Delta_{\rm asym}$) of the γ-ray transitions as obtained in this work for ^{63}Zn.

Level energy E_i(keV)	Gamma-ray energy[a] E_γ(keV)	Initial $\rightarrow$ final spin-parity $I_i^\pi \rightarrow I_f^\pi$	Relative intensity[f] I_γ	Branching ratio[g] B.R.	DCO ratio $R_{\rm DCO}$	Polarization asymmetry $\Delta_{\rm asym}$
192.94(8)	192.94	$5/2^- \rightarrow 3/2^-$	21.9(8)	100	0.56(8)[d]	
649.87(8)	456.93	$5/2^- \rightarrow 5/2^-$	1.91(6)	21.0(18)	1.02(34)[e]	
	649.87	$5/2^- \rightarrow 3/2^-$	16.5(7)	78.0(24)	0.48(8)[d]	0.03(11)
1063.20(7)	413.33	$7/2^- \rightarrow 5/2^-$	17.2(8)	19.0(6)	0.56(7)[d]	−0.02(8)
	870.26	$7/2^- \rightarrow 5/2^-$	13.78(72)	14.0(6)	0.83(19)[d]	−0.16(17)
	1063.20	$7/2^- \rightarrow 3/2^-$	100	66.8(12)	0.99(12)[d]	0.19(4)
1206.35(13)	1013.41	$7/2^- \rightarrow 5/2^-$	8.1(7)	50.2(23)	0.51(15)[d]	−0.25(22)
	1206.35	$7/2^- \rightarrow 3/2^-$	6.8(5)	49.8(24)	1.02(36)[d]	0.07(16)
1436.5(5)	1243.56[b]	$9/2^- \rightarrow 5/2^-$		100		
1702.98(11)	266.48[b]	$9/2^+ \rightarrow 9/2^-$	1.2(4)	1.2(4)		
	496.63	$9/2^+ \rightarrow 7/2^-$	13.2(7)	13.0(7)	0.71(11)[d]	−0.15(6)
	639.78	$9/2^+ \rightarrow 7/2^-$	109.3(23)	84.3(20)	0.50(4)[d]	0.01(5)
	1510.04[b]	$9/2^+ \rightarrow 5/2^-$	1.7(4)	2.0(4)		
2050.39(12)	987.19	$9/2^- \rightarrow 7/2^-$	12(1)	92(10)	1.37(72)[c]	
	1857.45[b]	$9/2^- \rightarrow 5/2^-$		8(3)		
2318.82(12)	1255.62	$11/2^- \rightarrow 7/2^-$	12.1(7)	100	0.98(37)[c]	
2585.23(15)	882.25	$13/2^+ \rightarrow 9/2^+$	78.8(24)	100	0.99(12)[c]	0.11(6)
2826.7(3)	1123.72	$11/2^{(+)} \rightarrow 9/2^+$	3.1(7)	100	1.67(67)[e]	
2934.6(6)	615.78[b]	$13/2^- \rightarrow 11/2^-$				
	1498.1[b]	$13/2^- \rightarrow 9/2^-$				
3357.5(6)	530.80[b]		1.60(58)	100		
3480.7(4)	654	$(13/2^+) \rightarrow 11/2^{(+)}$				
	1777.72	$13/2^+ \rightarrow 9/2^+$	2.4(6)			
3527.7(3)	1208.88[b]	$13/2^- \rightarrow 11/2^-$	2.2(6)	46(17)		
	1477.31[b]	$13/2^- \rightarrow 9/2^-$	3.0(7)	54(18)		
3764.11(17)	1178.88	$17/2^+ \rightarrow 13/2^+$	66.6(20)	100	0.97(11)[d]	0.15(6)
3769.91(17)	943.21[b]	$15/2^+ \rightarrow 11/2^{(+)}$	2.69(6)	35(9)		
	1184.68	$15/2^+ \rightarrow 13/2^+$	13.5(7)	65(16)	1.39(31)[d]	0.04(14)
4257.3(12)	899.80[b]			100		
4355.0(3)	590.89[b]	$(15/2^-) \rightarrow 17/2^+$	0.9(4)	8.0(36)[h]		
	874.30[b]	$(15/2^-) \rightarrow (13/2^+)$	1.9(6)	46(13)[h]		
	1769.77	$(15/2^-) \rightarrow 13/2^+$	6.3(6)	46(6)[h]	0.76(20)[d]	
4365.5(6)	595.59[b]		2.34(77)	100		
4684.2(8)	1326.70[b]		2.81(64)	100		
4776.2(6)	421.20[b]		1.79(70)	100		
5076.3(6)	721.30[b]		1.91(58)	100		
5076.6(3)	1306.69	$(19/2^+) \rightarrow 15/2^+$	5.6(10)	31(12)	1.0(5)[c]	
	1312.49	$(19/2^+) \rightarrow 17/2^+$	1.0(4)	69(18)	1.01(60)[c]	
5334.7(11)	1570.59[b]			100		
5346.06(20)	1581.95	$21/2^+ \rightarrow 17/2^+$	30.5(10)	100	0.97(12)[d]	0.16(5)
5406.5(4)	1878.80	$17/2^- \rightarrow 13/2^-$	1.3(5)		1.25(80)[c]	
	2471.90[b]	$17/2^- \rightarrow 13/2^-$				
5424.5(4)	1660.39[b]	$17/2^- \rightarrow 17/2^+$				
	1896.80[b]	$17/2^- \rightarrow 13/2^-$				
	2489.90[b]	$17/2^- \rightarrow 13/2^-$				
5916.1(3)	491.60[b]	$19/2^- \rightarrow 17/2^-$				
	509.60[b]	$19/2^- \rightarrow 17/2^-$	1.3(7)			
	570.04[b]	$19/2^- \rightarrow 21/2^+$	0.8(5)			
	1561.10[b]	$19/2^- \rightarrow 15/2^-$	1.8(4)			
6233.7(3)	317.60	$21/2^- \rightarrow 19/2^-$	1.8(5)	11.0(33)	0.68(34)[c]	
	809.20	$21/2^- \rightarrow 17/2^-$	7.6(7)	29.2(51)	1.78(1.25)[c]	
	827.20[b]	$21/2^- \rightarrow 17/2^-$	3.7(5)	37.9(62)		
	887.64[b]	$21/2^- \rightarrow 21/2^+$		15.8(42)		
	1157.17[b]	$21/2^- \rightarrow (19/2^+)$	1.00(36)	5.9(39)		
6385.5(6)	1039.44[b]		2.24(83)	100		

TABLE I. (*Continued.*)

Level energy E_i(keV)	Gamma-ray energy[a] E_γ(keV)	Initial → final spin-parity $I_i^\pi \rightarrow I_f^\pi$	Relative intensity[f] I_γ	Branching ratio[g] B.R.	DCO ratio R_{DCO}	Polarization asymmetry Δ_{asym}
6487.3(11)	1410.75[b]	$(23/2^+) \rightarrow (19/2^+)$		100		
6569.49(22)	335.79	$23/2^- \rightarrow 21/2^-$	0.8(4)	8.8(17)	0.76(33)[c]	
	653.39	$23/2^- \rightarrow 19/2^-$	2.84(47)	12.2(26)		
	1223.43	$23/2^- \rightarrow 21/2^+$	27.3(9)	79.0(35)	0.49(8)[d]	0.15(13)
7524.5(8)	1139.00[b]		2.23(43)	100		
7610.3(4)	1376.60[b]	$25/2^- \rightarrow 21/2^-$	3.9(8)	100		
7926.01(24)	1356.52	$27/2^{(-)} \rightarrow 23/2^-$	11.0(21)	100	0.83(18)[d]	
9095.8(8)	1485.50[b]	$(29/2^-) \rightarrow 25/2^-$				
	1169.79[b]	$(29/2^-) \rightarrow 27/2^{(-)}$				
9773.3(11)	1847.29[b]	$(31/2^-) \rightarrow 27/2^{(-)}$		100		
11048.3(9)	1952.50[b]		0.76(28)	100		

[a]The uncertainties lie between 0.1 and 0.5 keV depending upon the intensities.
[b]Estimation of R_{DCO} and Δ_{asym} was not possible due to the low intensities of the γ-ray transitions.
[c]Gate on $E2$, 1064 keV.
[d]Gate on $E2$, 882 keV.
[e]Gate on $E1$, 640 keV.
[f]The quoted error includes the fitting error plus a systematic error of 3% due to the uncertainties in efficiency and background subtraction.
[g]Branching ratios are derived by gating from above and measuring the intensities of depopulating transitions unless otherwise mentioned.
[h]Branching ratios are derived by gating from below and measuring the intensities of depopulating transitions.

of the 90° clover detectors used in the present experiment. It should be noted that a positive polarization asymmetry (Δ_{asym}) value implies the electric nature while a negative one implies the magnetic nature of the transition and a near zero value of $\Delta_{asym.}$ indicates that there is a strong admixture. The validity of this method is well verified by the known nature of the transitions in ^{63}Zn and the neighboring ^{64,66}Zn isotopes which were also populated in the fusion evaporation reaction. The polarization asymmetry values for the different γ-ray transitions of ^{63}Zn, as obtained in this work, are tabulated in Table I and plotted in Fig. 3.

III. RESULTS AND DISCUSSION

Based on the coincidence relationship, relative intensity, angular correlation, and polarization measurements we have proposed a new level scheme of ^{63}Zn. Here, almost all the previously reported transitions have been observed. New transitions observed in the present experiment are marked by asterisks in the level scheme (Fig. 4).

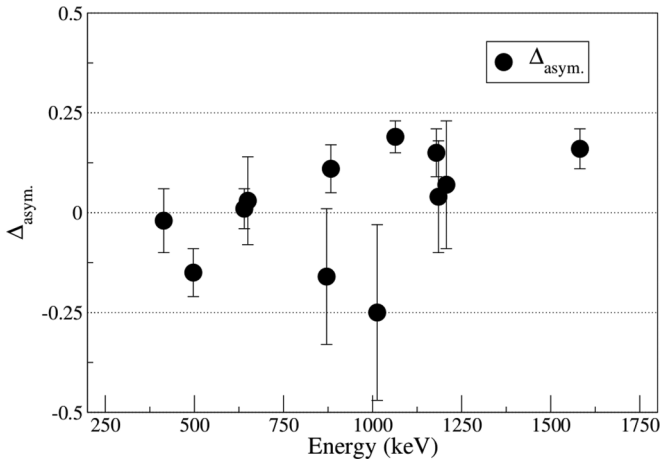

FIG. 3. Plot of polarization asymmetry values (Δ_{asym}) for different γ rays belonging to ^{63}Zn as obtained in this work.

A total of 13 new transitions have been observed and placed properly in the level scheme. Some of the previously known and new transitions are shown in the gated spectra (Figs. 5, 6, and 7). Ground state spin-parity of ^{63}Zn, as reported earlier, is $3/2^-$ which is fed by 1063 keV strong (B.R. $\approx$ 67%) γ ray from the 1063 keV, $7/2^-$ state. The measured DCO ratio and polarization asymmetry of this γ ray suggest that it is a stretched $E2$ type transition. The 1063 keV level also decays to 193 keV and 650 keV levels via emission of two strong (B.R. $\approx$ 14%) 870 keV and (B.R. $\approx$ 19%) 413 kev γ rays. The level at 193 keV, assigned with a spin-parity $5/2^-$, directly decays to the ground state via 193 keV transition with 100% branching. The measured DCO ratios and polarization asymmetries of 413 keV, 650 keV, and 1063 keV transitions suggest $5/2^-$ spin-parity value for the 650 keV state. The energy level at 1703 keV decays to the 1063 keV, 1206 keV, and 1437 keV levels via emission of 640 keV, 497 keV, and 266 keV γ rays and measured values of the DCO ratio and polarization asymmetry suggest a spin-parity value of $9/2^+$ for this state. A weak (B.R. $\approx$ 2%) 1510 keV γ-ray transition is observed between 1703 keV ($9/2^+$) and 193 keV ($5/2^-$) states and the spin-parity of these states suggest $M2$ nature of 1510 keV γ-ray transition. So it is very interesting to note that 1510 keV $M2$ transition is competing with two strong $E1$ transitions (640 keV and 497 keV). This transition was also observed by previous work [28]. Here, ^{65}Ge is another good example where a 1105 keV transition between $9/2^+$ and $5/2^-$ states was observed and angular distribution measurement confirmed its $M2$ character [5]. The level at 3770 keV decays to the $9/2^+$ level via the cascade of two

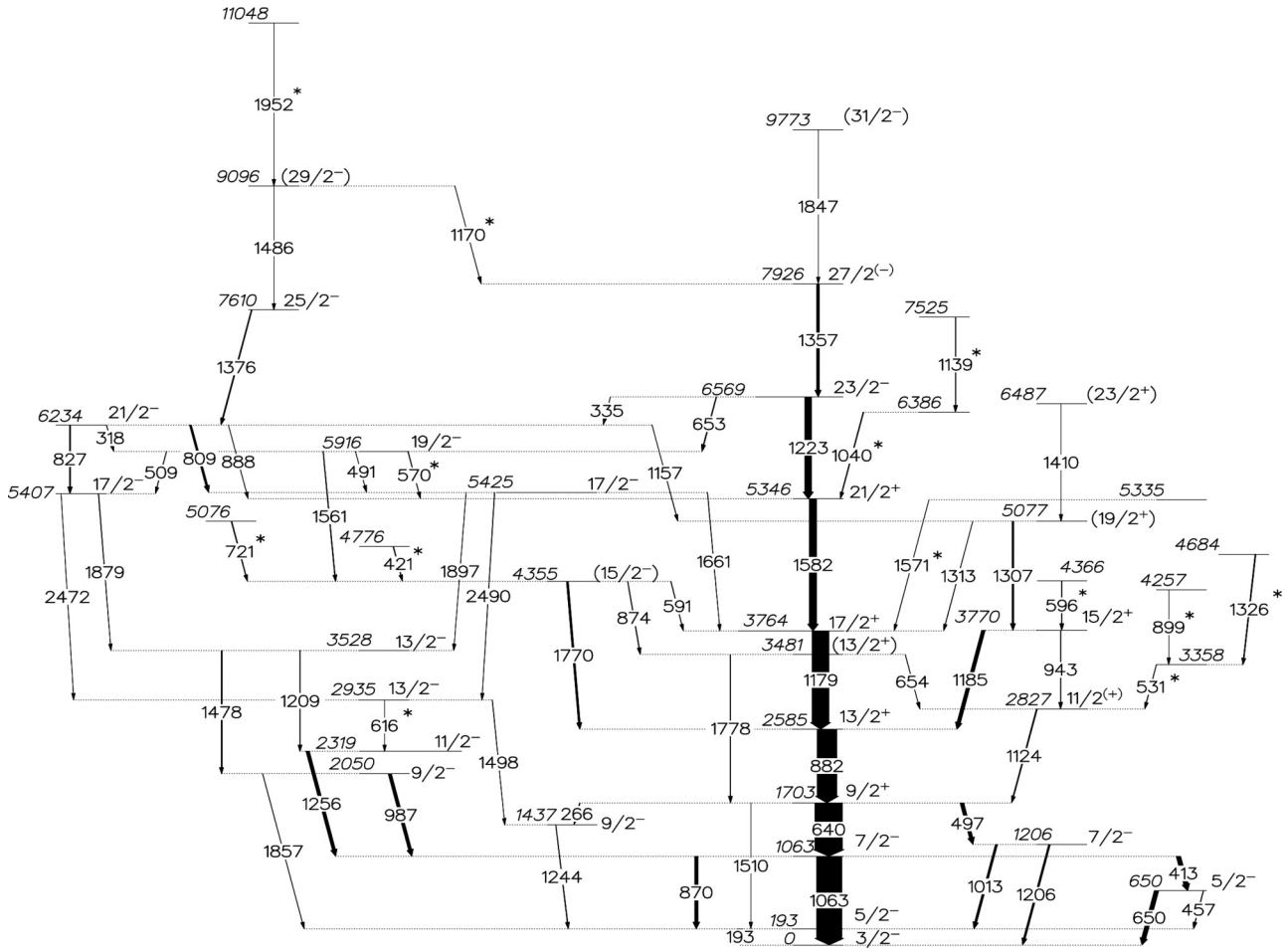

FIG. 4. Proposed level scheme of ^{63}Zn. Width of the arrows is proportional to the relative intensity of the respective transition observed in this experiment. The energies of the levels and γ rays are in keV.

strong (B.R. $\approx$ 65%) 1185 keV and (B.R. $\approx$ 100%) 882 keV γ rays. Measured values of the DCO ratio and polarization asymmetry suggest stretched electric quadrupole nature of 882 keV transition and mixed nature for 1185 keV. So, a spin-parity of $15/2^+$ is assigned for the 3770 keV state which

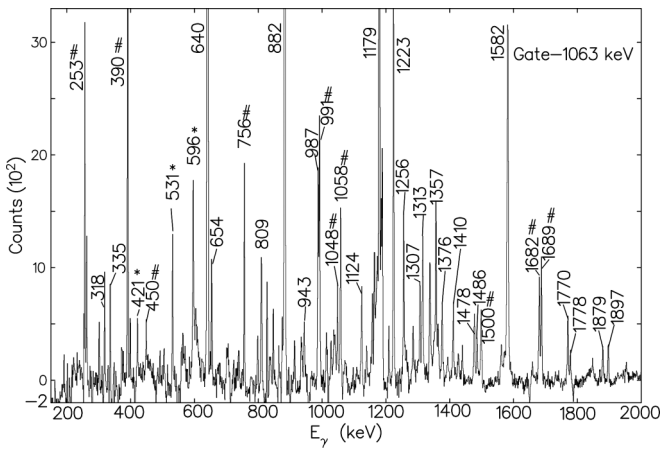

FIG. 5. Background subtracted γ-γ coincidence spectrum for ^{63}Zn gated on 1063 keV ($7/2^- \rightarrow 3/2^-$) transition. Here, y axis represents counts per 1.0 keV. New transitions are marked by asterisks (*) and contaminant peaks are identified with the # symbol.

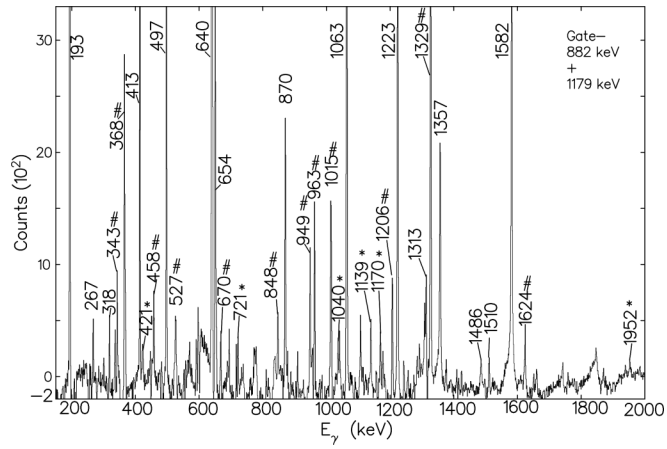

FIG. 6. Background subtracted γ-γ coincidence spectrum for ^{63}Zn in the sum gate of 882 keV ($13/2^+ \rightarrow 9/2^+$) + 1179 keV ($17/2^+ \rightarrow 13/2^+$) γ rays. Here, the y axis represents counts per 1.0 keV. New transitions are marked by asterisks (*) and contaminant peaks are identified with the # symbol.

was reported to be tentative in previous work. The measured values of DCO ratio and polarization asymmetry of 882 keV γ-ray transition confirm $13/2^+$ spin-parity value for the 2585 keV state, which is in disagreement with the assigned value of $3/2^-$ of a similar 2588 keV state reported by by Leach *et al.* [29]. As Leach *et al.* used a deuteron beam of 22 MeV for the reaction, high spin states of ^{63}Zn could not be populated in their work—so most of the high spin states observed in the current heavy-ion induced experiment, could not be compared with them. However, a few states which are close in energy values are compared. The $15/2^+$ state decays to the $9/2^+$ state via the cascade of 943 and 1124 keV γ rays. Three new levels with energies 3358, 4257, and 4684 keV have been added just above the 2827 keV, $11/2^{(+)}$ state. The 4257 keV state decays through the cascade of 899 keV and 531 keV γ rays and the 4684 keV state through 1326 keV and 531 keV γ rays to the 2827 keV level. Another level with energy 4366 keV has been placed into the level scheme just above the 3770 keV level which decays to the 3770 keV state via the emission of the 596 keV γ ray. Spin-parity assignment could not be done for these new 3358, 4257, 4366, and 4684 keV levels for low intensity of the emitted γ rays. These new levels with energy 3358, 4257, and 4684 keV can be compared respectively with 3365 ($7/2^-$), 4260 ($9/2^+$), and 4689 keV ($5/2^-$) states observed by Leach *et al.* The 3764 keV level decays to the 2585 keV level via the emission of a strong (B.R. $\approx$ 100%) 1179 kev γ ray, the measured values of the DCO ratio and polarization asymmetry suggest a spin-parity of $17/2^+$ to this 3764 keV state. Previous work by Leach *et al.*, identified many low excited states which were not populated in the recent heavy ion induced reaction and a comparative study shows that assigned spin-parity of 193 and 650 keV states exactly match with our observations. Leach *et al.* were not able to determine spin-parity of 1703 keV state—they used National Nuclear Data Center reported values. The newly observed 5335 keV state decays to this $17/2^+$ state via 1571 keV γ ray. The 6569 keV level decays to the 3764 kev state via the cascade of strong (B.R. $\approx$ 79%) 1223 keV and (B.R. $\approx$ 100%) 1582 keV γ rays. The measured values of DCO ratio and polarization asymmetry predict stretched electric quadrupole nature of 1582 keV and stretched electric dipole nature of the 1223 keV transition. The 5346 keV level is fed by two new transitions 1040 keV and 1139 keV in cascade, as observed in this experiment and are placed according to their coincidence relationship and relative intensity.

The negative parity $9/2^-$ and $11/2^-$ states having energy 2050 keV and 2319 keV, respectively, feed the 1063 keV state by 987 keV and 1256 keV transitions and the measured DCO ratios predict mixed nature for these two γ rays. These two low excited states were also observed by Leach *et al.*, but without any information about spin-parity. One new transition of energy 616 keV connecting the $13/2^-$ (2935 keV) and $11/2^-$ (2319 keV) states has been found in this work. Two new levels at 5076 keV and 4776 keV are added to the level scheme and they feed the tentatively assigned $15/2^-$ spin-parity state via 721 keV and 421 keV γ rays, respectively, and the decay of this $15/2^-$ state is fragmented into three γ rays, 591 keV (B.R. $\approx$ 8%) to the $17/2^+$ state, 874 keV (B.R. $\approx$ 46%) to the tentatively assigned $13/2^+$ state, and

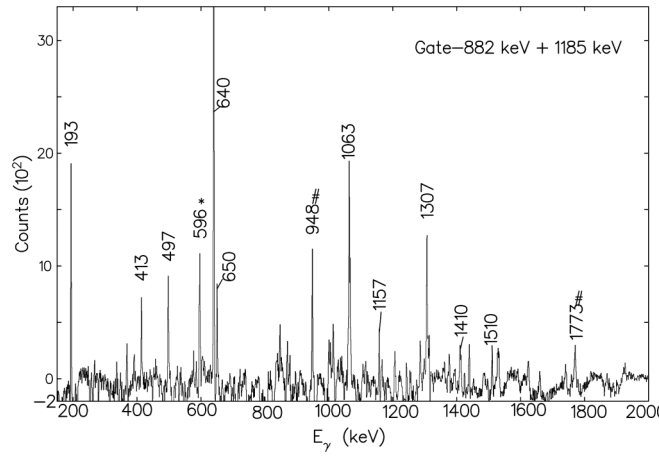

FIG. 7. Background subtracted γ-γ coincidence spectrum for ^{63}Zn in the sum gate of 882 keV ($13/2^+ \rightarrow 9/2^+$) + 1185 keV ($15/2^+ \rightarrow 13/2^+$) γ rays. Here, the y axis represents counts per 1.0 keV. New transitions are marked by asterisks (*) and contaminant peaks are identified with the # symbol.

1770 keV (B.R. $\approx$ 46%) to the $13/2^+_1$ state. The 5916 keV $19/2^-$ level decays to 5425 ($17/2^-$), 5346 ($21/2^+$), and 5407 keV ($17/2^-$) levels by 491, 570, and 509 keV γ rays, respectively. Here, the 570 keV γ ray is a new transition observed in this work. The 6234 keV level with spin-parity $21/2^-$ decays via 318 (B.R. $\approx$ 11%), 809 (B.R. $\approx$ 29%), 827 (B.R. $\approx$ 38%), 888 (B.R. $\approx$ 16%), and 1157 (B.R. $\approx$ 6%) keV transitions to both positive parity and negative parity states and is fed by the 1376 keV (100% branching) γ ray from 7610 keV state with spin-parity $25/2^-$. So, the energy level $21/2^-$ at 6234 keV decays mostly by fragmented γ rays. The fragmented decay pattern as observed in some of the negative parity states indicates that the corresponding wave functions are of highly complex nature. A new transition of 1952 keV has also been observed and is placed above the 9096 keV state which feeds the 7610 keV level via the 1486 keV γ ray. The 1170 keV transition is a new transition that connects the 9096 keV state having a tentative spin-parity $29/2^-$ to the 7926 keV $27/2^{(-)}$ state. The placement of the 1952 keV γ ray extends the level scheme up to 11 MeV. The energy states above $31/2^-$ are inaccessible in this experiment and this is probably due to the presence of long-lived isomers above this spin and excitation energy or may be due to the incomplete fusion caused by the loss of input angular momentum in this reaction. Also we cannot ignore the sharing of γ-ray yield because of the large density of states at such high excitation energy but a more obvious reason may be the limited sensitivity of the setup we used, which could not permit us to observe highly nonyrast states that were populated in the reaction. More access to higher spin ($>31/2\hbar$) states could have been gained by improving the sensitivity of the setup with the help of ancillary devices, such as the charged particle array along with the full INGA array consisting of 24 clover detectors.

A. Shell model calculations

Calculations on even-A Zn isotopes using anharmonic vibrator model [42,43] are able to explain many interesting

phenomena emerging out of lower excitations successfully. The structure of low lying levels in odd-mass isotopes of Zn is explained in terms of the coupling of the odd single particle to the vibrating core [44]. Quasiparticle-phonon coupling model was used by Weidinger [45] and by Throop [46] in order to understand the experimental decay scheme of ^{65}Zn and ^{67}Zn, respectively. Shell model calculations for ^{64,66,68}Zn with model space consisting of $p_{3/2}$, $f_{5/2}$, and $p_{1/2}$ orbitals outside the closed ^{56}Ni core, along with an effective Hamiltonian from Koops and Glaudemans, were done by Van Hienen *et al.* [47]. A comparison of quasiparticle-core coupling and shell model calculations with experiment exhibited very good agreement for low lying negative parity states for both ^{65}Zn and ^{67}Zn but a lack of similarity was observed for higher excited states. Similar situation arises for ^{63}Zn [27] with same model space and interaction.

In order to understand the observed nuclear structure in ^{63}Zn, shell model calculations have been performed in the present work using the interaction jj44bpn [48]. The shell-model code NUSHELLX [49] is used for this purpose. With the ^{56}Ni core, the valence space for the calculation consists of $2p_{3/2}$, $1f_{5/2}$, $2p_{1/2}$, and $1g_{9/2}$ proton and neutron orbitals. Here, the effective Hamiltonian jj44bpn, due to Brown and Lesitskiy [48], is a realistic interaction based on the Bonn-C potential, which has been obtained by fitting binding energies and excitation energies in the Ni, Cu, and Zn isotopes and nuclei close to $N = 50$. Previous calculations for ^{60,62,64,66}Zn [50] and ^{63}Cu [32] by Rai *et al.*, with the similar interaction and model space have produced very good agreements. The single particle energies for the $2p_{3/2}$, $1f_{5/2}$, $2p_{1/2}$, and $1g_{9/2}$ orbitals are taken to be 9.6566, 9.2859, 8.2695, and 5.8944 MeV, respectively. Reduced transition probabilities [$B(E2)$ values] have been calculated for the $21/2^+ \rightarrow 17/2^+$, $17/2^+ \rightarrow 13/2^+$, and $13/2^+ \rightarrow 9/2^+$ transitions using standard effective charges $e_p = 1.5\,e$ and $e_n = 0.5\,e$ and the calculated values are 11.81, 16.69, and 17.38 Weisskopf unit (W.u.), respectively. While taking the half-lives from Ref. [26] and using the experimental B.R. of the present work, we have obtained experimental $B(E2)$ values for $21/2^+ \rightarrow 17/2^+$, $17/2^+ \rightarrow 13/2^+$, and $13/2^+ \rightarrow 9/2^+$ transitions which are (>)14, 78 (23), and 20 (2) W.u., respectively. So shell model calculations for the transitions $21/2^+ \rightarrow 17/2^+$ and $13/2^+ \rightarrow 9/2^+$ produce near similar $B(E2)$ values as obtained from experiment but it is unable to reproduce the large collectivity [indicated by large $B(E2)$ value] for the transition $17/2^+ \rightarrow 13/2^+$. A comparison of the calculated energy levels with the experimental results shows overall good agreement for both parity states as shown in Fig. 8. All the energy states calculated by the shell model and labeled in Fig. 8 are of lowest energy values corresponding to the given spin-parity. The comparison is made here, only for the states having exactly measured or tentatively assigned spin-parity, therefore, experimentally observed levels, which do not have any assigned spin-parity, are not compared with the shell model calculation.

Spin and parity of ground state and first excited state are predicted correctly by jj44bpn interaction which are $3/2^-$ and $5/2^-$, respectively. While the energies of these two states are correctly predicted, that of second excited $5/2^-$ state is

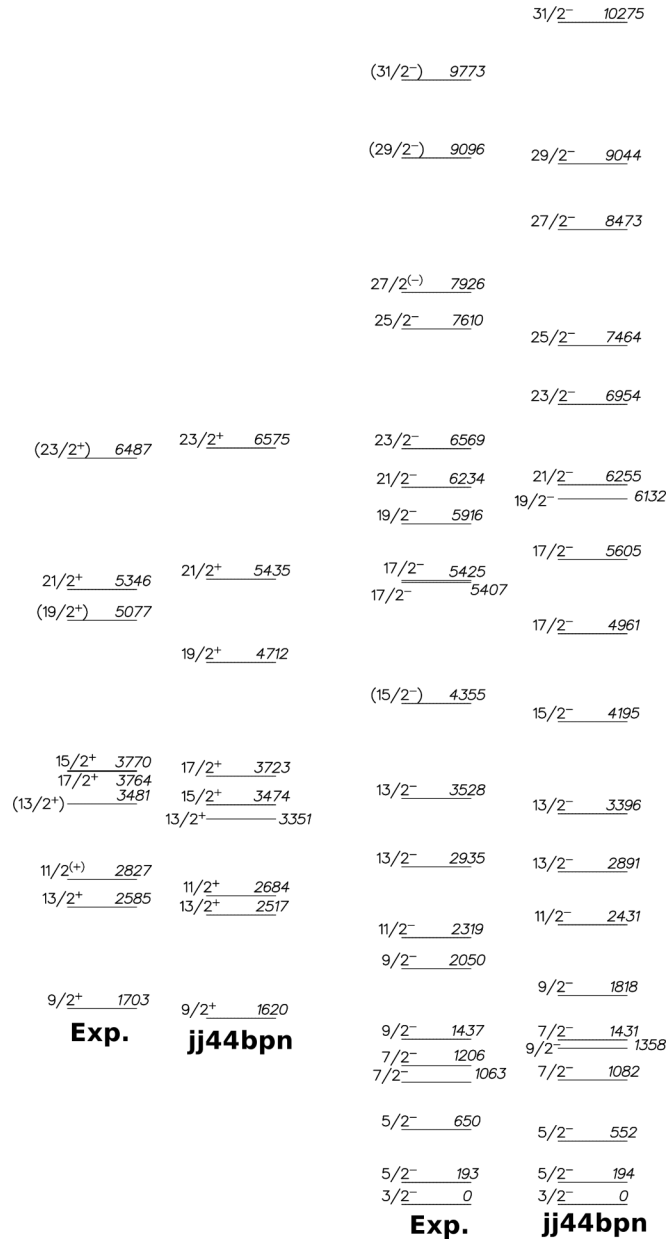

FIG. 8. Comparison of the shell model calculated level energies using the jj44bpn [48] interaction with the experimental values. The negative parity and the positive parity states are shown separately. The number on the left of the level represents the spin (in $\hbar$)-parity and that on the right represents the level energy in keV.

underpredicted by ≈ 100 keV. Very good matching between theory and experiment is observed for first $7/2^-$ and $9/2^-$ states, while that for the second excited $7/2^-$ state is over predicted and $9/2^-$ state is under predicted in the model. For the lower and moderate excitation energies a very good agreement between the calculated energies and experimental values is observed. For few high spin negative parity states lack of agreement is also observed. Similarly for all positive parity states from $9/2^+$ up to $23/2^+$, almost all the energy levels (with the exception of a little discrepancy for the $15/2^+$ and $19/2^+$ states) are reproduced well by the model

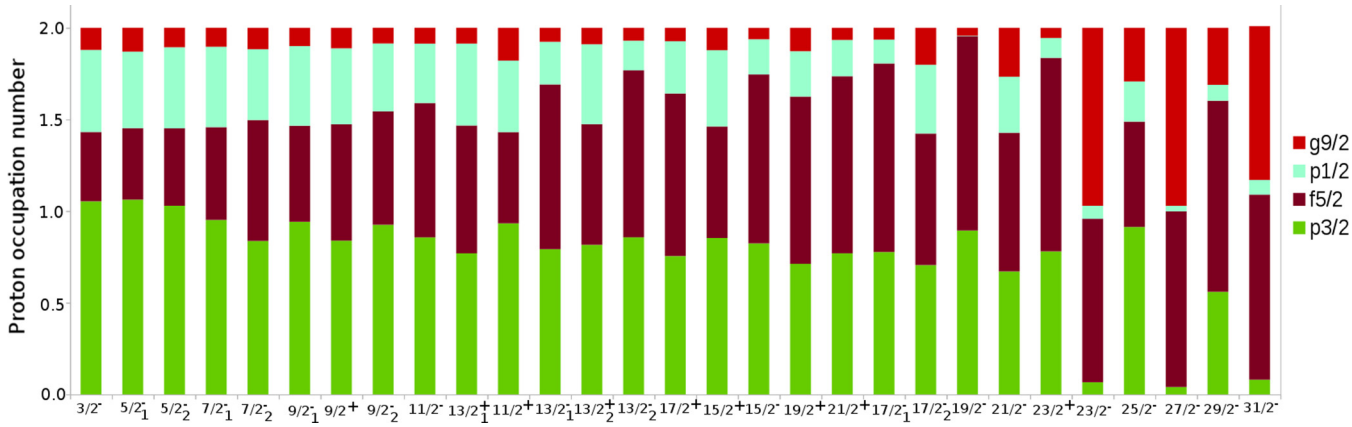

FIG. 9. Calculated occupation probabilities of the $p_{3/2}$, $f_{5/2}$, $p_{1/2}$, and $g_{9/2}$ orbitals for the proton in ^{63}Zn. The occupation probabilities are calculated from the shell model calculation using the jj44bpn interaction.

with the chosen interaction and model space. We have also calculated occupation probabilities for proton and neutron in the same model space and Hamiltonian. An occupation probability gives the strength of individual contribution of different orbitals ($2p_{3/2}$, $1f_{5/2}$, $2p_{1/2}$, and $1g_{9/2}$ in the case of present calculation) of both the proton and neutron in total wave function. So this calculation is important as it gives information regarding the structure of different levels. From the occupation number plots (Figs. 9 and 10), major contributions from the $p_{3/2}$ and $f_{5/2}$ orbitals to both kind of parity states are clearly evident. For $23/2^-$, $25/2^-$, and $27/2^-$ states, a large contribution in total wave function is coming from the intruder $1g_{9/2}$ orbital. Moreover, shell model calculations can not predict properly the energy values of $23/2^-$, $27/2^-$, and $31/2^-$ negative parity states. It indicates that origin of these states are different and may be due to the particle excitation from $f_{7/2}$ to $g_{9/2}$ orbital. The important role of $f_{7/2}$ holes in developing collective bands in neighboring Zn isotopes is well known. Most notable fact is that for all the positive parity states, the contribution of the $1g_{9/2}$ neutron in the total wave function is significant. Hence, a variety of structural effects are expected due to this shape driving the $g_{9/2}$ orbital. So in order to investigate the possibility of collective nature and evolution of shapes we have done potential energy calculations for ^{63}Zn.

B. TRS calculation

The total Routhian surface (TRS) in a fixed quasiparticle configuration is defined as a sum of Strunisky energy and the rotational energy. Here, Strunisky energy contains liquid drop plus shell correction terms. Configuration is specified in terms of parity (π), signature (α), and excitation quantum numbers. We have performed TRS calculations for ^{63}Zn using the Hartree-Fock-Bogoliubov code of Nazarewich *et al.* [51,52] for a single quasineutron in the $g_{9/2}$ orbital. Equilibrium shapes were calculated in the (β_2, γ) plane at each rotational frequency ($\hbar\omega$) minimizing with respect to β_4. Here, β_2, γ, and β_4 represent quadrupole deformation, triaxiality, and hexadecapole deformation parameters, respectively. As a residual interaction, the monopole pairing force has been taken with the strength from Ref. [52]. Here, the calculation

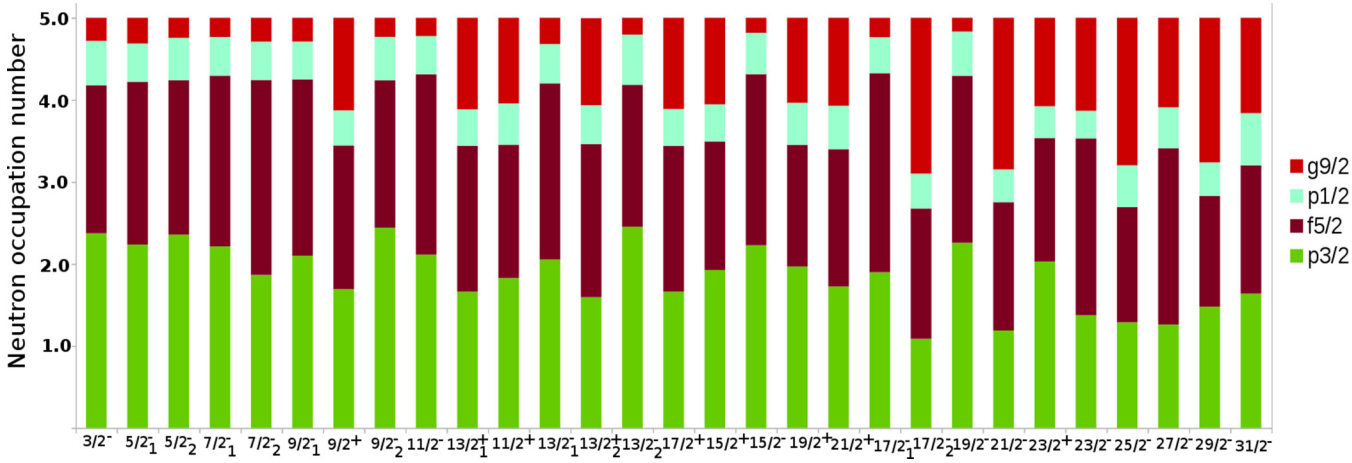

FIG. 10. Calculated occupation probabilities of the $p_{3/2}$, $f_{5/2}$, $p_{1/2}$, and $g_{9/2}$ orbitals for the neutron in ^{63}Zn. The occupation probabilities are calculated from the shell model calculation using the jj44bpn interaction.

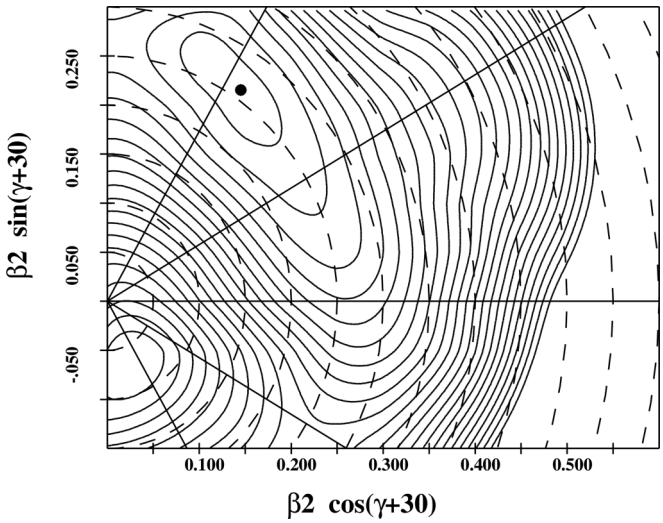

FIG. 11. TRS plot for ^{63}Zn for $(\pi, \alpha = +, +1/2)$ configuration at $\hbar\omega = 0.30$ MeV. Contours are 250 keV apart from each other. The shape corresponding to the energy minima is predicted to be triaxial ($\gamma \approx 23^\circ$) with $\beta_2 \approx 0.25$.

for positive parity and positive signature predicts collective triaxial shape with quadrupole deformation $\beta_2 \approx 0.25$ and triaxiality parameter $\gamma \approx 23^\circ$ for both $\hbar\omega$ values (i.e., at 0.30 MeV and 0.40 MeV) as shown in Figs. 11 and 12. Calculations at higher $\hbar\omega$ value (≈ 0.65 MeV) showed very near collective prolate shapes with $\gamma \approx 5^\circ$ and at a large value of quadrupole deformation $\beta_2 \approx 0.45$ (Fig. 13).

TRS calculations with a $g_{9/2}$ quasineutron predict the presence of collective triaxial deformed shape at low rotational frequency with moderate value of β_2. It evolves to an enhanced collective prolate structure with the increase in rotational frequency. Though signs of such large deformation

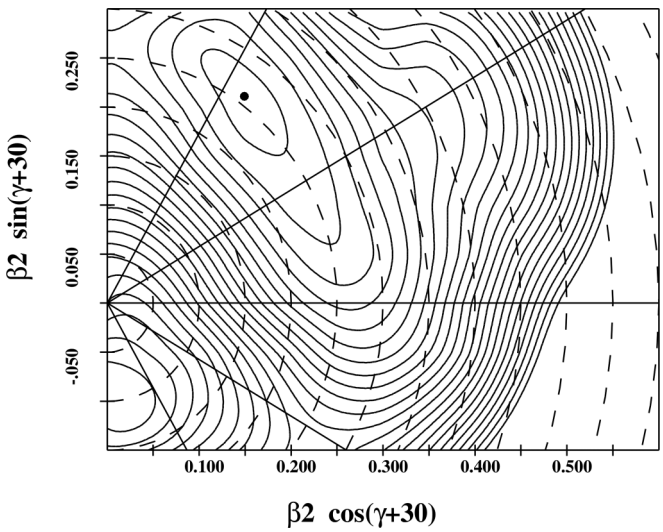

FIG. 12. Same as Fig. 11 at $\hbar\omega = 0.40$ MeV. The shape corresponding to the energy minima is predicted to be triaxial with almost similar values of the triaxiality and quadrupole deformation parameters as at 0.30 MeV.

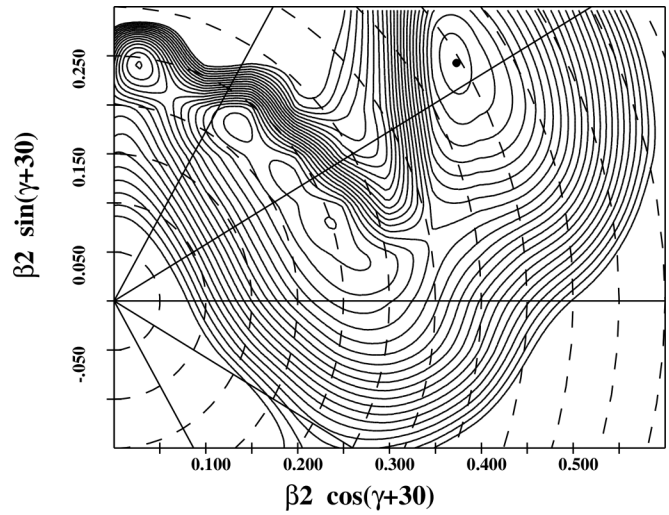

FIG. 13. Same as Fig. 11 at $\hbar\omega = 0.60$ MeV. The shape corresponding to the energy minima is predicted to be near prolate ($\gamma \approx 5^\circ$) with $\beta_2 \approx 0.45$.

($\beta_2 \approx 0.45$) as predicted by TRS could not be confirmed by the present experiment but further investigation is required in future to search for large collectivity at such large deformation.

IV. CONCLUSIONS

In the present work with an efficient array of clover detectors we have observed 13 new transitions and ten new levels in ^{63}Zn. The level scheme is extended up to an excitation energy of ≈ 11 MeV. Multipolarity of many transitions with their electric or magnetic nature has been established adequately by DCO and polarization measurement. Shell model calculations are performed in the $f_{5/2}pg_{9/2}$ model space with the ^{56}Ni core using the effective interaction jj44bpn to interpret the obtained level structure of this nucleus. A reasonable agreement is found to exist between the observed level structure and the results from the shell model calculations. With an improved set of the two-body matrix elements and incorporating the full $fpg_{9/2}$ model space, i.e., including the $1f_{7/2}$ orbital for calculations, a more accurate description may be obtained. Total Routhian surface calculations predict collective excitation with triaxial and prolate shape at moderate and large value of deformation parameter (β_2), respectively.

ACKNOWLEDGMENTS

We would like to acknowledge the support from the Pelletron staff of IUAC for providing an excellent beam and INGA collaborators for loan of detectors. Support from target laboratory and from D. Kanjilal, IUAC is highly acknowledged. We would like to thank S. Nandi (VECC), S. S. Bhattacharjee (IUAC), and R. Garg (IUAC) for their help during the experiment. We would also like to acknowledge the financial supports from SERB/DST (New Delhi) with File No. EMR/2015/000891 and IUAC (New Delhi) with

File No. UFR-49318. We are grateful to the Nuclear Data Review Group at NNDC, Brookhaven National Laboratory, for the data consistency check on the manuscript and the least-squares fit calculation of the level energies.

[1] P. J. Emnis *et al.*, Nucl. Phys. A **535**, 392 (1992).
[2] A. P. de Lima *et al.*, Phys. Rev. C **23**, 213 (1981).
[3] L. Chaturvedi *et al.*, Phys. Rev. C **43**, 2541 (1991).
[4] U. Hermkens *et al.*, Z. Phys. A **343**, 371 (1992).
[5] U. Hermkens *et al.*, Phys. Rev. C **52**, 1783 (1995).
[6] D. Rudolph *et al.*, Phys. Rev. Lett. **80**, 3018 (1998).
[7] C. Andreoiu *et al.*, Phys. Rev. C **62**, 051301(R) (2000).
[8] L. L. Anderson *et al.*, Eur. Phys. J. A **36**, 251 (2008).
[9] B. Mukherjee, S. Muralithar, R. P. Singh, R. Kumar, K. Rani, and R. K. Bhowmik, Phys. Rev. C **63**, 057302 (2001).
[10] C. Andreoiu *et al.*, Eur. Phys. J. A **14**, 317 (2002).
[11] W. Nazarewicz *et al.*, Nucl. Phys. A **429**, 269 (1984).
[12] W. Nazarewicz, Nucl. Phys. A **520**, 333c (1990).
[13] C. E. Svensson *et al.*, Phys. Rev. Lett. **82**, 3400 (1999).
[14] C.-H. Yu, C. Baktash, J. Dobaczewski, J. A. Cameron, C. Chitu, M. Devlin, J. Eberth, A. Galindo-Uribarri, D. S. Haslip, D. R. LaFosse, T. J. Lampman, I. Y. Lee, F. Lerma, A. O. Macchiavelli, S. D. Paul, D. C. Radford, D. Rudolph, D. G. Sarantites, C. E. Svensson, J. C. Waddington, and J. N. Wilson, Phys. Rev. C **60**, 031305(R) (1999).
[15] L.-L. Andersson *et al.*, Eur. Phys. J. A **30**, 381 (2006).
[16] L.-L. Andersson *et al.*, Phys. Rev. C **79**, 024312 (2009).
[17] A. Galindo-Uribarri *et al.*, Phys. Lett. B **422**, 45 (1998).
[18] D. Karlgren *et al.*, Phys. Rev. C **69**, 034330 (2004).
[19] A. V. Afanasjev, D. B. Fossan, G. J. Lane, and I. Ragnarsson, Phys. Rep. **322**, 1 (1999).
[20] C. E. Svensson *et al.*, Phys. Rev. Lett. **79**, 1233 (1997).
[21] C. E. Svensson *et al.*, Phys. Rev. Lett. **80**, 2558 (1998).
[22] J. Gellanki *et al.*, Phys. Rev. C **86**, 034304 (2012).
[23] C. H. Yu, C. Baktash, J. Dobaczewski, J. A. Cameron, M. Devlin, J. Eberth, A. Galindo-Uribarri, D. S. Haslip, D. R. LaFosse, T. J. Lampman, I. Y. Lee, F. Lerma, A. O. Macchiavelli, S. D. Paul, D. C. Radford, D. Rudolph, D. G. Sarantites, C. E. Svensson, J. C. Waddington, and J. N. Wilson, Phys. Rev. C **62**, 041301(R) (2000).
[24] B. Mukherjee, S. Muralithar, R. P. Singh, R. Kumar, K. Rani, R. K. Bhowmik, and S. C. Pancholi, Phys. Rev. C **64**, 024304 (2001).
[25] O. M. Mustaffa *et al.*, J. Phys. G **4**, 99 (1978).
[26] O. M. Mustaffa *et al.*, J. Phys. G **5**, 1283 (1979).
[27] P. A. S. Metford, T. Taylor, and A. Cameron, Nucl. Phys. A **308**, 210 (1978).
[28] A. K. Singh *et al.*, Phys. Rev. C **57**, 1617 (1998).
[29] K. G. Leach *et al.*, Phys. Rev. C **87**, 064306 (2013).
[30] G. K. Mehta *et al.*, Nucl. Instrum. Methods Phys. Res. A **268**, 334 (1988).
[31] S. Muralithar *et al.*, Nucl. Instrum. Methods Phys. Res. A **622**, 281 (2010).
[32] S. Rai *et al.*, Eur. Phys. J. A **54**, 84 (2018).
[33] U. S. Ghosh *et al.*, in *Proceedings of the DAE Symposium on Nuclear Physics 63* (Department of Atomic Energy, Government of India, 2018), p. 130.
[34] B. P. Ajith Kumar *et al.*, in *Proceedings of the 44th DAE-BRNS Symposium on Nuclear Physics* (Department of Atomic Energy, Government of India, 2001), p. 390.
[35] D. C. Radford, Nucl. Instrum. Methods Phys. Res., Sect. A **361**, 297 (1995).
[36] R. K. Bhowmik *et al.*, in [34], p. 422.
[37] K. S. Krane *et al.*, Nucl. Data Tables **11**, 351 (1973).
[38] G. Duchene *et al.*, Nucl. Instrum. Methods Phys. Res. A **432**, 90 (1999).
[39] K. Starosta *et al.*, Nucl. Instrum. Methods Phys. Res. A **423**, 16 (1999).
[40] S. Chakraborty *et al.*, Braz. J. Phys. **47**, 406 (2017).
[41] R. Palit *et al.*, Pramana J. Phys. **54**, 347 (2000).
[42] L. S. Kisslinger and K. Kumar, Phys. Rev. Lett. **19**, 1239 (1967).
[43] J. W. Lightbody, Jr., Phys. Lett. B **38**, 475 (1972).
[44] V. K. Thankappan and W. W. True, Phys. Rev. **137**, B793 (1965).
[45] A. Weidinger, E. Finckh, U. Jahnke, and B. Schreiber, Nucl. Phys. A **149**, 241 (1970).
[46] M. J. Throop, Y. T. Cheng, and D. K. McDaniels, Nucl. Phys. A **239**, 333 (1975).
[47] J. F. A. Van Hienen *et al.*, Nucl. Phys. A **269**, 159 (1976).
[48] A. F. Lisetskiy, B. A. Brown, M. Horoi, and H. Grawe, Phys. Rev. C **70**, 044314 (2004).
[49] A. Brown and W. D. M. Rae, Nucl. Data Sheets **120**, 115 (2014).
[50] S. Rai *et al.*, Int. J. Mod. Phys. E **25**, 11 (2016).
[51] W. Nazarewicz *et al.*, Nucl. Phys. A **512**, 61 (1990).
[52] W. Nazarevricz, J. Dudek, R. Bengtsson, T. Bengtsson, and I. Ragnarsson, Nucl. Phys. A **435**, 397 (1985).